

Anti-CIAS1/NALP3/NLRP3 Antibody Picoband®

Catalog Number: PA1665

About NLRP3

NLRP3 (NLR FAMILY, PYRIN DOMAIN-CONTAINING 3), also known as CIAS1, CRYOPYRIN, NALP3 or PYPAF1, is a protein that in humans is encoded by the NLRP3 (NOD-like receptor family, pyrin domain containing 3) gene. The NLRP3 gene encodes a pyrin-like protein expressed predominantly in peripheral blood leukocytes. And the NLRP3 gene is mapped on 1q44. NLRP3 interacts with apoptosis-associated speck-like protein containing a CARD (ASC). The encoded protein may play a role in the regulation of inflammation and apoptosis. Mutation of the NALP3 nucleotide-binding domain reduced ATP binding, CASP1 activation, IL1B production, cell death, macromolecular complex formation, self-association, and association with ASC. Consistent with an essential role for Nlrp3 inflammasomes in antifungal immunity, Gross et al. showed that Nlrp3-deficient mice are hypersusceptible to *C. albicans* infection. Activation of the NLRP3 inflammasome in response to virus or to RNA was dependent upon lysosomal maturation and reactive oxygen species production in human cells. The NLRP3 inflammasome senses obesity-associated danger signals and contributes to obesity-induced inflammation and insulin resistance.

Overview

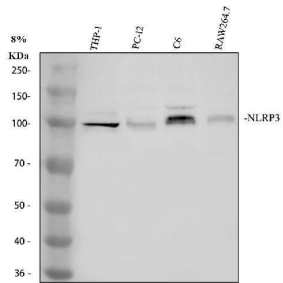
Product Name	Anti-CIAS1/NALP3/NLRP3 Antibody Picoband®
Reactive Species	Human, Mouse, Rat
Description	Boster Bio Anti-CIAS1/NALP3/NLRP3 Antibody catalog # PA1665. Tested in IHC, WB applications. This antibody reacts with Human, Mouse, Rat. The brand Picoband indicates this is a premium antibody that guarantees superior quality, high affinity, and strong signals with minimal background in Western blot applications. Only our best-performing antibodies are designated as Picoband, ensuring unmatched performance.
Application	Flow Cytometry, IHC, WB
Clonality	Polyclonal
Formulation	Each vial contains 4 mg Trehalose, 0.9 mg NaCl and 0.2 mg Na ₂ HPO ₄ .
Storage Instructions	Store at -20°C for one year from date of receipt. After reconstitution, at 4°C for one month. It can also be aliquotted and stored frozen at -20°C for six months. Avoid repeated freeze-thaw cycles.
Host	Rabbit
Uniprot ID	Q96P20

Technical Details

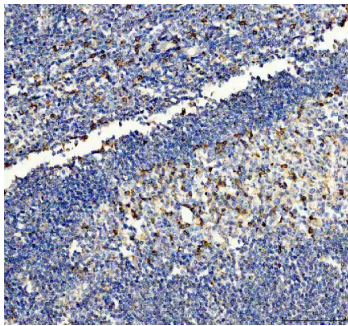
Immunogen	A synthetic peptide corresponding to a sequence at the N-terminus of human CIAS1, different from the related rat and mouse sequences by one amino acid.
Recommended Detection Systems	Boster recommends Enhanced Chemiluminescent Kit with anti-Rabbit IgG (EK1002) for Western blot, and HRP Conjugated anti-Rabbit IgG Super Vision Assay Kit (SV0002-1) for IHC(P).
Cross Reactivity	No cross-reactivity with other proteins

Isotype	Rabbit IgG
Form	Lyophilized
Concentration	Adding 0.2 ml of distilled water will yield a concentration of 500 ug/ml.
Purification	Immunogen affinity purified.
Suggested Dilutions	Western blot, 0.1-0.5ug/ml, Human, Mouse, Rat Immunohistochemistry (Paraffin-embedded Section), 2-5ug/ml, Human

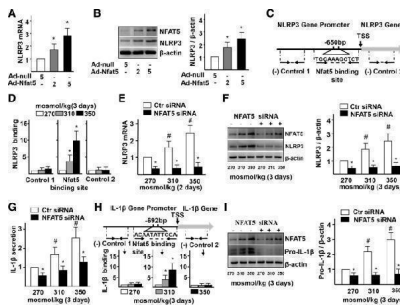
Anti-CIAS1/NALP3/NLRP3 Antibody Picoband® (PA1665) Images



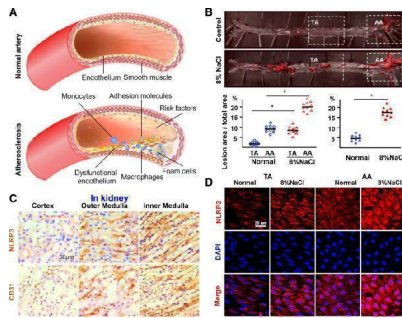
Western blot analysis of NLRP3 using anti-NLRP3 antibody (PA1665). Electrophoresis was performed on a 8% SDS-PAGE gel at 80V (Stacking gel) / 120V (Resolving gel) for 2 hours. The sample well of each lane was loaded with 30 ug of sample under reducing conditions. Lane 1: human THP-1 whole cell lysates, Lane 2: rat PC-12 whole cell lysates, Lane 3: rat C6 whole cell lysates, Lane 4: mouse RAW264.7 whole cell lysates. After electrophoresis, proteins were transferred to a nitrocellulose membrane at 150 mA for 50-90 minutes. Blocked the membrane with 5% non-fat milk/TBS for 1.5 hour at RT. The membrane was incubated with rabbit anti-NLRP3 antigen affinity purified polyclonal antibody (PA1665) at 0.5 ug/mL overnight at 4°C, then washed with TBS-0.1%Tween 3 times with 5 minutes each and probed with a goat anti-rabbit IgG-HRP secondary antibody (Catalog # BA1054) at a dilution of 1:5000 for 1.5 hour at RT. The signal is developed using an ECL Plus Western Blotting Substrate (Catalog # AR1196-200) with Tanon 5200 system. A specific band was detected for NLRP3 at approximately 100-110 kDa. The expected band size for NLRP3 is at 118 kDa.



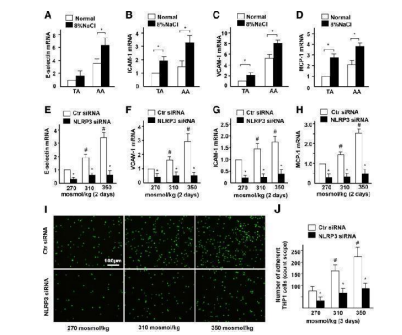
IHC analysis of NLRP3 using anti-NLRP3 antibody (PA1665). NLRP3 was detected in a paraffin-embedded section of human tonsil tissue. Heat mediated antigen retrieval was performed in EDTA buffer (pH 8.0, epitope retrieval solution). The tissue section was blocked with 10% goat serum. The tissue section was then incubated with 2 ug/ml rabbit anti-NLRP3 Antibody (PA1665) overnight at 4°C. Peroxidase Conjugated Goat Anti-rabbit IgG was used as secondary antibody and incubated for 30 minutes at 37°C. The tissue section was developed using HRP Conjugated Rabbit IgG Super Vision Assay Kit (Catalog # SV0002) with DAB as the chromogen.



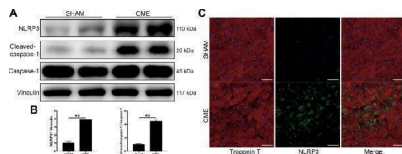
High-salt-elevated NFAT5 mediates transcription of NLRP3 and IL-1 β in ECs. a-b mRNA and protein levels of NLRP3 in ECs treated with Adenovirus-null (Ad-null, 5 MOI) and Adenovirus-NFAT5 (Ad-NFAT5, 2 MOI or 5 MOI). c-d High-salt increases binding of NFAT5 to the promoter region of IL-1 β . Diagram showing the region of the NFAT5 binding site upstream of the transcription start site (TSS) of NLRP3, and the regions that were used to analyze NFAT5 binding by ChIP. ChIP results are relative to 270 mosmol/kg. e-f mRNA and protein levels of NLRP3 in ECs treated with high-salt and transfected with Ctr siRNA or NFAT5 siRNA. g Protein secretion of IL-1 β in ECs treated with high-salt and transfected with Ctr siRNA or NFAT5 siRNA. h High-salt increases binding of NFAT5 to the promoter region of IL-1 β . i Protein levels of pro-IL-1 β in ECs treated with high-salt and transfected with Ctr siRNA or NFAT5 siRNA. All data were presented as mean \pm SEM, N \geq 3. * p



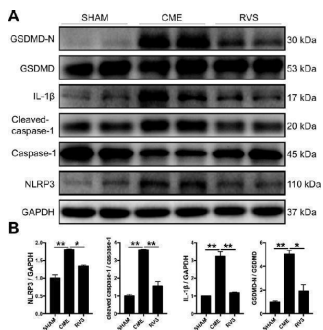
High-salt intake predisposes atherosclerosis and upregulates NLRP3 expression. a Schematic shows the process of atherosclerosis formation. b Oil Red O staining of aortas and quantification of percentage lesion areas in the thoracic aorta (TA) and aortic arch (AA) of ApoE ^{-/-} mice (n = 10) fed with a normal or high-salt diet for 12 weeks. c Immunohistochemistry staining for NLRP3 and CD31 in the kidney at 4 weeks. Nuclei, hematoxylin staining. d En face immunofluorescent staining of NLRP3 of ECs in TA and AA of ApoE^{-/-} mice fed with a normal or high-salt diet for 4 weeks. See Additional file : Figure S1D for NLRP3 mRNA qPCR. All data were presented as mean ± SEM, N ≥ 9. * p



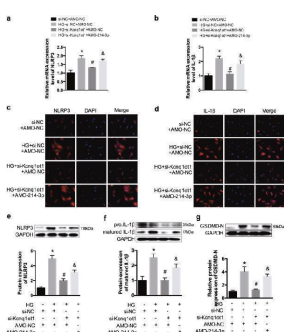
High-salt elevates endothelial inflammation via NLRP3. a-d Quantification of mRNA levels of E-selectin, ICAM-1, VCAM-1 and MCP-1 in TA and AA of ApoE^{-/-} mice fed with a normal or high-salt diet. e-h Quantification of mRNA levels of E-selectin, VCAM-1, ICAM-1, and MCP-1 in ECs treated with high-salt and transfected with Control siRNA or NLRP3 siRNA. i, j The adhesion of Calcein-labeled THP-1 monocytes in ECs treated with high-salt and transfected with Control siRNA or NLRP3 siRNA. All data were presented as mean ± SEM, N ≥ 3. * p



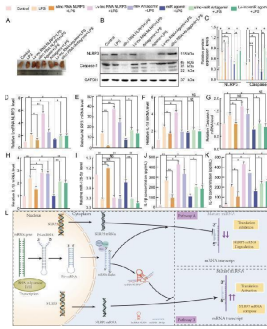
NLRP3 and cleaved-caspase-1 are upregulated in mice heart 3 days after CME intervention. A Representative immunoblots of NLRP3 and cleaved-caspase-1 expression in sham and CME mice hearts. B Densitometric analysis of relative protein expressions, Vinculin is used as loading control. n = 4 per group. Data represent the mean ± SEM of three replicates. C Representative images of immunofluorescent double staining of Troponin T and NLRP3 in cardiac tissues. Scale bars = 50 μm. n = 4 per group. * P



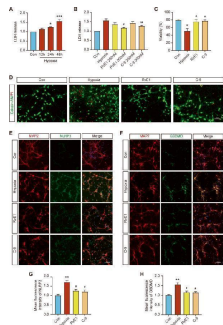
RVS restrains the activation of the NLRP3 inflammasome at 3 days after CME intervention. A Representative immunoblots for myocardial NLRP3, caspase-1, cleaved-caspase-1, IL-1beta, GSDMD, GSDMD-N in the hearts of sham, CME and RVS-treated mice. B The densitometric analysis of relative protein expressions, GAPDH is used as loading control. n = 4 per group. Data represent the mean ± SEM of three replicates. * P



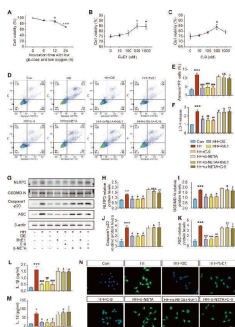
The texts overlap in figure 6g. So I want to replace it with a new in the attachment. Kcnq1ot1/miR-214-3p pathway regulates inflammation in fibroblasts a, b qRT-PCR was conducted to detect expression of NLRP3 and IL-1beta. c, d The expression levels of NLRP3 and IL-1beta were determined by immunofluorescence. e - g Western blot was performed to determine the expression of NLRP3, IL-1beta, and GSDMD-N. * P



The mechanism by which the lncRNA NLRP3/miR-138-5p/NLRP3 ceRNA network functions in the inflammatory response. The lungs of rats were injected with PBS in the control group and LPS-treated rats were further treated with si-r-lncRNA NLRP3, Lv-lncRNA NLRP3, agomiR-138-5p, antagomiR-138-5p, Lv-lncRNA NLRP3 + agomiR-138-5p, and si-r-lnc NLRP3 + antagomiR-138-5p. A Morphometric changes in the appearance of the lungs that had been fixed in 4% paraformaldehyde for 24 h at 25 °C in each group. B , C The protein expression levels of NLRP3 and caspase-1 in rat lung tissues. qRT-PCR assays were used to analyse mRNA expression of D lncRNA NLRP3, E NLRP3, F IL-18, G Caspase-1, H IL-1β, and I miR-138-5p in the lung tissues of rats. ELISA analysis of the IL-1β (J) and IL-18 (K) levels in the culture supernatant. L Graphical summary of the role of the lncRNA NLRP3/miR-138-5p/NLRP3 ceRNA network in acute lung injury. beta-Actin was used as the reference. The data are presented as mean ± SE (n = 6). * P

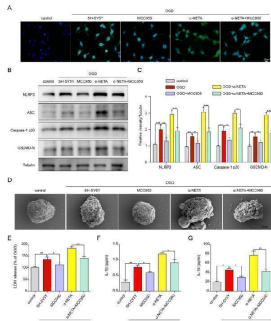


ChemR23 activation ameliorated pyroptosis after chronic hypoxic stimulation in primary rat hippocampal neurons. A Changes in LDH release in the cell culture supernatant with time under hypoxic conditions. n = 4 per group. B Effects of different concentrations of RvE1 and C-9 on the release of LDH in primary neurons under hypoxic stimulation. n = 4 per group. C Cell viability of each group under different treatment conditions. n = 3 per group. D Fluorescence images of primary neurons stained with calcein AM (live cells, green fluorescence) and PI (dead cells, red fluorescence) after different treatments. Scale bar: 50 μm. n = 3 per group. E Double immunostaining of NLRP3 with MAP2 in primary neurons of different groups. Scale bar: 100 μm. n = 3 for each group. F Double immunostaining of GSDMD with MAP2 in primary neurons of different groups. Scale bar: 100 μm. n = 3 for each group. G The statistics of the mean fluorescence intensity of NLRP3 in each group. n = 3 for each group. H The statistics of the mean fluorescence intensity of GSDMD in each group. n = 3 for each group. Data are presented as the mean ± SEM. *P<0.05, **P<0.01, ***P<0.001 vs. Con; #P<0.05, ##P<0.01 vs. Hypoxia. Index in PubMed under a CC BY license. PMID: 37932279

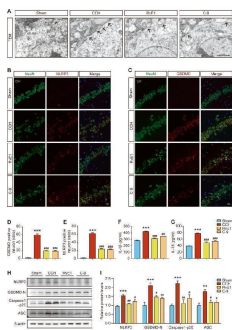


Effects of ChemR23 activation on pyroptosis in SH-SY5Y cells after hypoglycaemic and hypoxic stimulation. A Changes in cell viability with time under hypoglycaemic and hypoxic conditions. n = 4 per group. B , C Effects of different concentrations of RvE1 and C-9 on cell viability. n = 4 per group. D , E The proportion of Annexin V/PI double positive cells analysed by flow cytometry. n = 3 per group. F LDH levels in the cell culture supernatant. n = 3 per group. G - K Western blot analysis of NLRP3, GSDMD-N, Caspase-1 p20 and ASC. n = 3 per group. L , M Concentrations of IL-1β and IL-18 in the cell culture supernatant were measured by ELISA. n = 4 per group. (N) Representative immunofluorescence staining of NLRP3 (green) with the nuclei counterstained by DAPI. Scale bar: 50 μm. n = 3 per group. Data are presented as the mean ± SEM. **P<0.01,

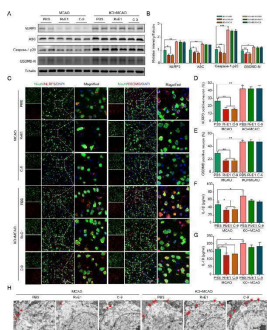
***P<0.001 vs. Con; #P<0.05, ##P<0.01, ###P<0.001 vs. HH; &P<0.05, &&P<0.01, &&&P<0.001 vs. HH+RvE1; †P<0.05, ††P<0.01, †††P<0.001 vs. HH + C-9. Index in PubMed under a CC BY license. PMID: 37932279



The neuroprotective effect of ChemR23 against OGD-induced neuronal pyroptosis was NLRP3 dependent. A Representative immunofluorescent images of NLRP3 in cultured neurons. Scale bar = 20 μ m. B , C Immunoblots and quantitative analysis of NLRP3, ASC, caspase-1 p20, GSDMD-N in treated neurons after OGD. D Representative scanning electron microscopy pictures of neurons. Scale bar = 10 μ m. E LDH release was assessed and quantified in neurons subjected to OGD for 4 h. F , G ELISA analysis for IL-1 β and IL-18 levels in supernatants of neuron subjected to OGD for 4 h. At least three independent experiments were repeated. Data are represented as mean \pm SD. *P<0.05, **P<0.01, ***P<0.001 Index in PubMed under a CC BY license. PMID: 38178174

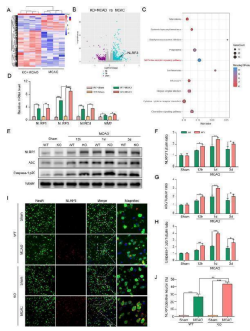


Effects of ChemR23 activation with RvE1 or C-9 on neuronal pyroptosis in CCH rats. A Representative transmission electron micrographs of hippocampal neurons in different treatment groups. Black arrowhead: membrane pores. Scale bar: 2 μ m. n = 3 per group. B , C Representative double immunofluorescence staining of GSDMD/NeuN and NLRP3/NeuN in the rat hippocampus. Scale bar: 20 μ m. n = 3 per group. D , E Quantitative statistics of GSDMD/NeuN or NLRP3/NeuN double-positive cells in rat hippocampus. n = 3 per group. F , G ELISA results of IL-1 and IL-18 analysis in the rat hippocampus. n = 4 per group. H , I Representative immunoblotting bands and the expression levels of NLRP3, GSDMD-N, Caspase-1 p20 and ASC in the rat hippocampus. n = 4 per group. Data are presented as the mean \pm SEM. **P<0.01, ***P<0.001 vs. sham; #P<0.05, ##P<0.01, ###P<0.001 vs. CCH. Index in PubMed under a CC BY license. PMID: 37932279

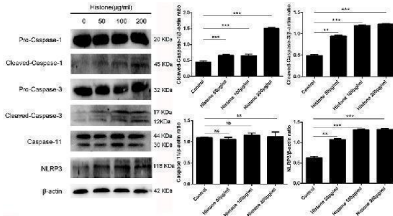


RvE1 and C-9 ameliorated NLRP3 inflammasome-mediated pyroptosis in MCAO mice. A , B Immunoblots and quantitative analysis of NLRP3, ASC, caspase-1 p20, GSDMD-N (n = 3/per group). C - E Double immunofluorescent staining of NLRP3 or GSDMD with NeuN in ischemic penumbra region and quantitative analysis at Day 1 after MCAO (n = 3/per group). Scale bar = 20 μ m. F , G The ELISA assays for IL-1 β and IL-18 levels in ipsilateral brain tissues subjected to ischemia at Day 1 (n = 4/per group). H Representative microphotographs and quantification of neuronal death based on NeuN and TUNEL assay in the ischemic ipsilateral brain regions at Day 1 after MCAO (n = 3/per group). Scale bar = 2 μ m. Data are represented as mean \pm SD. *P<0.05, **P<0.01, ***P<0.001 Index in PubMed under a CC BY license. PMID: 38178174

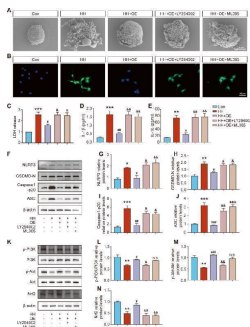
ChemR23 deletion amplified NLRP3 inflammasome activation in cerebral ischemia injury. A , B Thermograms



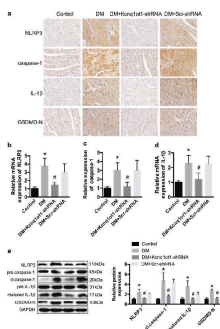
and volcano plots showing the comparison between ChemR23 KO group and WT group at Day 1 after MCAO (n = 4/per group). C The KEGG pathway enrichment analysis (n = 4/per group). D qPCR analysis of the infammasome sensor genes NLRP1, NLRP3, NLRC4, and AIM2 ipsilateral hemispheres of WT mice and KO mice subjected to MCAO at Day 1 (n = 3/per group). E - H Western blotting and quantitative analysis of NLRP3, ASC, caspase-1 p20 expression in ischemic penumbra tissue at 12 h, Day 1 and Day 3 after MCAO (n = 3/per group). I, J Representative immunofluorescence staining images of NLRP3 were co-stained with NeuN in peri-infarct areas and their quantification at Day 1 after MCAO (n = 3/per group). Scale bar = 20 um. Data are represented as mean ± SD. *P<0.05, **P<0.01, ***P<0.001 Index in PubMed under a CC BY license. PMID: 38178174



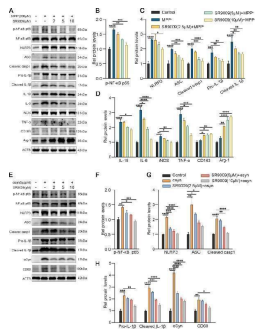
Histone induce BMECs pyroptosis is dependent on activations of caspase 1, caspase 3 and NLRP3. BMECs were incubated with stimulated histone for 16 h, and the activities of these proteins were determined by western blotting. Data are presented as mean ± SEM (n = 5). P-values of < 0.05 were considered significant (** P < 0.01, *** P < 0.001, and "ns" means not significant). Index in PubMed under a CC BY license. PMID: 31156617



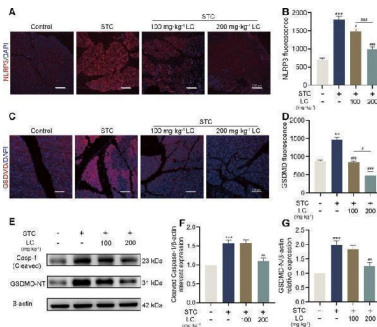
ChemR23 activation inhibited neuronal pyroptosis via the PI3K/AKT/Nrf2 signalling pathway in SH-SY5Y cells. A Scanning electron microscopy analysis showing the cell morphology in different treatment groups. n = 3 per group. B Representative immunofluorescence staining of NLRP3 (green) with the nuclei counterstained by DAPI. Scale bar: 50 um. n = 3 per group. C LDH levels in the cell culture supernatant. n = 3 per group. D, E ELISA of IL-1beta and IL-18 levels. n = 3 per group. F - J The levels of NLRP3, GSDMD-N, Caspase-1 p20 and ASC were evaluated by western blot. n = 3 per group. K - N The expression levels of p-PI3K/PI3K, p-AKT/AKT and Nrf2 were evaluated by western blot. n = 3 per group. Data are presented as the mean ± SEM. *P<0.05, **P<0.01, ***P<0.001 vs. Con; #P<0.05, ##P<0.01, ###P<0.001 vs. HH; &P<0.05, &&P<0.01, &&&P<0.001 vs. HH + OE; N.S. means not significant vs. HH + OE. Index in PubMed under a CC BY license. PMID: 37932279



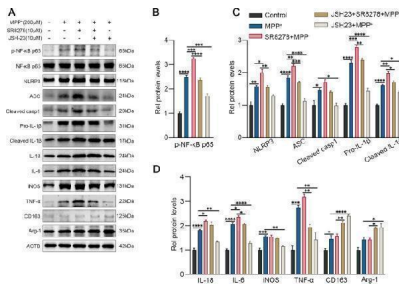
Kcnq1ot1 is involved in the regulation of pyroptosis in vivo a Immunohistochemistry analysis was performed to detect the expression NLRP3, caspase-1, IL-1beta, and GSDMD-N. Scale bar, 20 um. b - d qRT-PCR was conducted to analyze the mRNA expression of NLRP3, caspase-1 and IL-1beta. e Western blot was conducted to determine the protein expression of NLRP3, caspase-1 and IL-1beta. * P



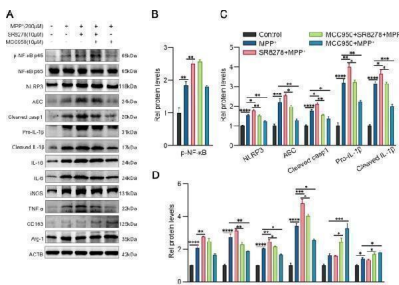
Activation of Rev-erbalpha inhibited microglial activation induced by MPP + and alphasyn PFF. The representative western blot bands (A) and the statistical graph (B - D) of p-NF-kappaB p65, NLRP3, ASC, cleaved caspase-1, IL-1beta, IL-18, IL-6, TNF-a, iNOS, Arg-1 and CD163 protein expressions. BV2 cells were pretreated with SR9009 (2 uM, 5 uM, 10 uM) for 1 h, then incubated with MPP + for 24 h. The representative western blot bands (E) and the statistical graph (F-H) of p-NF-kappaB p65, NLRP3, ASC, cleaved caspase-1, IL-1beta, CD68 and alphasyn protein expressions. BV2 cells were pretreated with SR9009 (2 uM, 5 uM, 10 uM) for 1 h, then incubated with alphasyn preformed-fibril for 6 h. The p-NF-kappaB p65 level was normalized to the total of NF-kappaB p65, and the rest protein levels were normalized to beta-actin. Data were presented as mean ± SEM (n = 3). (* p



CPT1A protects against SAP in mice by inhibiting the NLRP3/GSDMD-mediated pyroptosis signalling pathway. (A-D) Immunofluorescence staining of NLRP3 and GSDMD in the pancreas of mice received different treatments. Scale bar: 100 um. (E-G) Protein levels of cleaved Caspase-1 and GSDMD-NT in the pancreas of mice received different treatments. beta-actin served as the loading control. All data are presented as means ± SEM, n = 3-5. * p < 0.05, ** p < 0.01, *** p < 0.001 vs. Control group. # p < 0.05, ## p < 0.01, ### p < 0.001 vs. STC group. & p < 0.05, && p < 0.001 vs. LC (100 mg/kg) treatment group. Index in PubMed under a CC BY license. PMID: 40718711

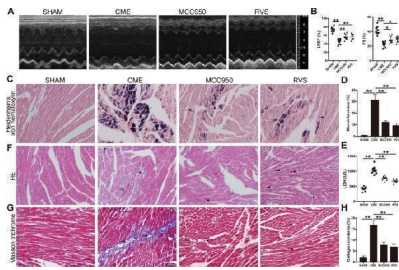


Rev-erbalpha regulates microglial activation by NF-kappaB inflammasome pathway. The representative western blot bands (A) and the statistical graph (B - D) of p-NF-kappaB p65, NLRP3, ASC, cleaved caspase-1, IL-1beta, IL-18, IL-6, TNF-a, iNOS, Arg-1 and CD163 protein expressions. BV2 cells were pretreated with JSH-23 (10 uM) or SR8278 (10 uM) for 1 h, then incubated with MPP + for 24 h. The p-NF-kappaB p65 level was normalized to the total of NF-kappaB p65, and the rest protein levels were normalized to beta-actin. Data were presented as mean ± SEM (n = 3). (* p

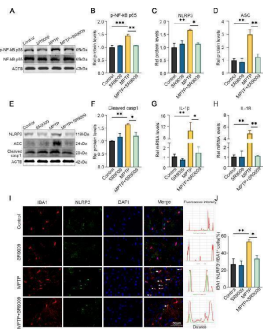


Rev-erbalpha regulates microglial activation by NLRP3 inflammasome pathway. The representative western blot bands (A) and the statistical graph (B - D) of p-NF-kappaB p65, NLRP3, ASC, cleaved caspase-1, IL-1beta, IL-18, IL-6, TNF-a, iNOS, Arg-1 and CD163 protein expressions. BV2 cells were pretreated with MCC950 (10 uM) or SR8278 (10 uM) for 1 h, then incubated with MPP + for 24 h. The p-NF-kappaB p65 level was normalized to the total of NF-kappaB p65, and the rest protein levels were normalized to beta-actin. Data were presented as mean ± SEM (n = 3). (* p

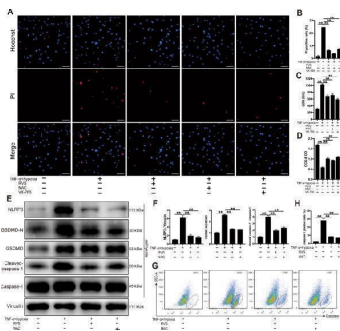
MCC950 and RVS protect against CME-induced cardiac dysfunction and injury. A Representative M-mode echocardiograms for each group at 3 days after CME intervention. Mice were treated with RVS and the selective



NLRP3 inflammasome inhibitor MCC950 three days prior and after CME intervention at 40 and 20 mg/kg/d respectively. **B** Left ventricular ejection fraction (LVEF) and fractional shortening (FS) are measured using Doppler echocardiography. $n = 8$ to 10 per group. Data represent the mean \pm SEM. **C** Representative images of Heidenhain's iron hematoxylin staining for each group to visualize microinfarct areas, the microinfarct areas are stained into dark gray. **D** The quantitative analysis of microinfarct areas. $n = 8$ to 10 per group. The quantification is representative of the percentage of microinfarct area in 5 fields \pm SEM by random. **E** Serum lactate dehydrogenase (LDH) levels are measured in each group. $n = 8$ to 10 per group. Data represent the mean \pm SEM. **F** Representative images of HE staining to visualize the local micro-infracted lesions for each group. **G** Representative images of Masson trichrome staining of the ventricular sections of each group. **H** The quantitative analysis of collagen contents. $n = 8$ to 10 per group. The quantification is representative of the percentage of collagen contents in 5 fields \pm SEM by random. Scale bars = $50 \mu\text{m}$. Black arrows indicate the microspheres. * P

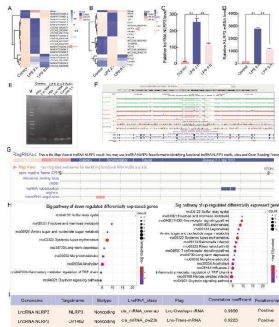


SR9009 suppresses NLRP3 inflammasome activation in the SN of MPTP-induced mice. The representative western blot bands (**A**) and the statistical graph (**B**) of p-NF-kappaB p65 and NF-kappaB p65 in the SN. The representative western blot bands (**E**) and the statistical graph (**C - D**, **F**) of NLRP3, ASC and cleaved-caspase-1 in the SN. The real-time PCR results of IL-1beta (**G**) and IL-18 (**H**) in the SN. **I** Representative double-immunofluorescent staining of IBA1 (red) and NLRP3 (green) in the SN and the statistical graph (**J**) of IBA1 + /NLRP3 + /IBA1 + cells. Scale bar, $50 \mu\text{m}$. $n = 3-4$ for each group. The p-NF-kappaB p65 level was normalized to the total of NF-kappaB p65, and the rest protein levels were normalized to beta-actin. Data were presented as mean \pm SEM. (* p

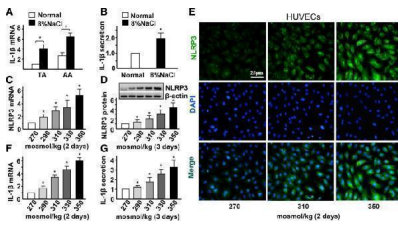


RVS and ROS scavenger inhibit the activation of the NLRP3 inflammasome and pyroptosis in H9c2 cells. **A** The H9c2 cells are stimulated with 40 ng/ml TNF-alpha combined with hypoxia for 12 h to activate the NLRP3 inflammasome. The caspase-1 selective inhibitor VX-765 and ROS scavenger N-acetylcysteine (NAC) are added 2 h before the stimulation at $20 \mu\text{M}$ and 5 mM respectively. The pyroptotic cells are determined by Hoechst 33342/PI staining, wherein the nuclei are stained to blue by Hoechst 33342, and the pyroptotic cells are stained to red by PI. Scale bars = $50 \mu\text{m}$. **B** The quantitative analysis of PI positive cells. $n = 6$ per group. The quantification is representative of the percentage of pyroptotic cells in 5 fields \pm SEM by random. **C** LDH release is measured by a cytotoxicity detection LDH kit. $n = 6$ per group. **D** Cell viability is measured by a CCK-8 kit, and the optical densities (ODs) are compared among the groups. $n = 6$ per group. **E** Representative immunoblots for NLRP3, caspase-1, cleaved-caspase-1, GSDMD, GSDMD-N in H9c2 cells. **F** The densitometric analysis of relative protein expressions. Vinculin is used as a loading control. $n = 4$ per group. **G** Cells with active caspase-1 in each group are

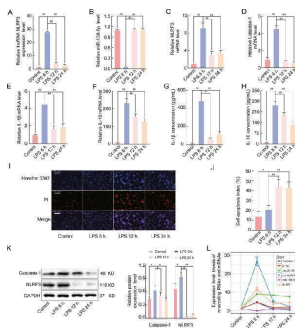
stained with FLICA (FAM-YVAD-FMK) probe and detected using flow cytometer. H The percentages of caspase-1 positive cells are compared among the groups. n = 6 per group. Data represent the mean ± SEM. All experiments were repeated three times. * P



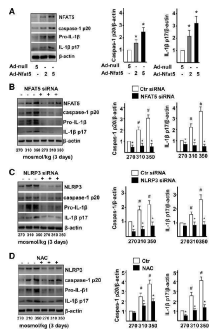
Dysregulated transcription of lncRNA NLRP3 and NLRP3 in LPS-treated NR8383 AM cells as determined by RNA-seq and bioinformatics analysis. A The heat map lists the top 20 differentially expressed lncRNAs and mRNAs in NR8383 AM after treatment with PBS, LPS for 2 h, and LPS for 9 h. A , B RNA-seq analysis shows the quantified gene expression of lncRNA NLRP3 and NLRP3 in AM cells in the negative control, LPS 2 h, and LPS 9 h groups. C , D Agarose gel electrophoresis analysis shows the quantified expression of lncRNA NLRP3 and NLRP3 in NR8383 cells. beta-Actin served as the control. E The conservation of lncRNA NLRP3 was predicted and analysed by the UCSC Genome Browser. F The lncRNA NLRP3 potential protein-coding and binding sites were analysed with RNA 2.0 tools. G The results show that lncRNA NLRP3 has no protein-coding capability. H Gene Ontology and Kyoto Encyclopedia of Genes and Genomes pathway analysis were used to analyze differentially expressed genes. I The relationship between lncRNA NLRP3 and NLRP3, and the correlation coefficient is listed. * P



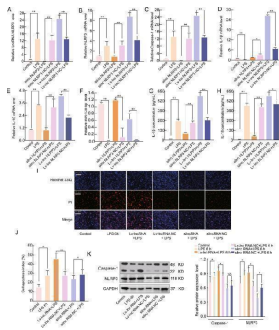
High-salt enhances NLRP3 inflammasome activation in ECs. a Quantification of mRNA levels of IL-1beta in TA and AA of ApoE ^{-/-} mice fed with a normal or high-salt diet for 4 weeks. b Quantification of protein levels of IL-1beta in the serum of ApoE ^{-/-} mice fed with a normal or high-salt diet for 4 weeks. c, d Quantification of mRNA levels and protein levels of NLRP3 by HUVECs in hypertonic medium (290, 310, 330 and 350 mosmol/kg) with isomolar 270 mosmol/kg as the control, evaluated by RT-qPCR and Western blotting with beta-actin as the internal control. e Immunofluorescent staining of NLRP3 in HUVECs with iso- and hyper-osmotic media. f, g mRNA and protein expression of IL-1beta in HUVECs exposed to iso- and hyper-osmotic media, evaluated by RT-qPCR and ELISA. All data were presented as mean ± SEM, N ≥ 3. * p



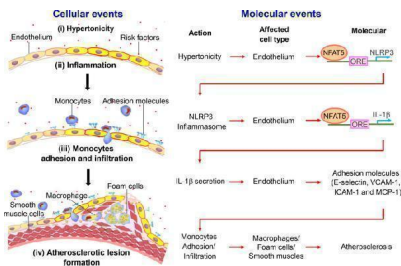
Effects of LPS on the lncRNA NLRP3, miR-138-5p, NLRP3, Caspase-1, IL-1beta, and IL-18 expression levels in early ALI. A qRT-PCR assay was used to analyse the mRNA expression of A lncRNA NLRP3, B miR-138-5p, C NLRP3, D Caspase-1, E IL-1beta, and F IL-18 in LPS-induced ALI. beta-Actin was used as the reference gene. G , H ELISA analysis of the IL-1beta and IL-18 levels in the culture supernatant. Cell apoptosis was determined by Hoechst 33342 and PI dual staining assays (I) and counted (J). The expression of NLRP3 and caspase-1 in the NR8383 AM cells from the four groups was analysed by western blotting (K). L Expression trends of lncRNA NLRP3, NLRP3, caspase-1, IL-1beta, IL-18, and miR-138-5p in the negative control group and groups treated with LPS for 6, 12, and 24 h. The data are presented as mean ± SE (n = 6). * P



High-salt activates NLRP3 inflammasome in ECs via NFAT5. a Immunoblot of NFAT5, caspase-1 p20, pro-IL-1beta, and IL-1beta p17, and quantification of caspase-1 activity and mature IL-1beta in ECs treated with Adenovirus-null (Ad-null, 5 MOI) and Adenovirus-NFAT5 (Ad-NFAT5, 2 MOI or 5 MOI). See Additional file : Figure S4 for caspase-1 activity. b Immunoblot images of NFAT5, caspase-1 p20, pro-IL-1beta, and IL-1beta p17, and quantification of active caspase-1 and mature IL-1beta in ECs treated with high-salt and transfected with Ctr siRNA or NFAT5 siRNA. c Immunoblot images of NLRP3, caspase-1 p20, pro-IL-1beta, and IL-1beta p17, and quantification of active caspase-1 and mature IL-1beta in ECs treated with high-salt and transfected with Ctr siRNA or NLRP3 siRNA. d Immunoblot images of NLRP3, caspase-1 p20, pro-IL-1beta, and IL-1beta p17, and quantification of active caspase-1 and mature IL-1beta in ECs treated with high-salt, treated with NAC. All data were presented as mean \pm SEM, N \geq 3. * p

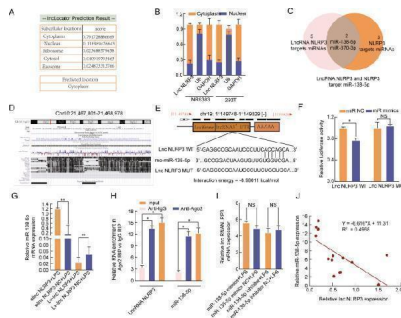


LncRNA NLRP3 regulates the inflammatory response during ALI through NLRP3 inflammasomes. A qRT-PCR assay was used to analyse the mRNA expression of A lncRNA NLRP3, B NLRP3, C Caspase-1, D IL-18, E IL-1beta, and F miR-138-5p in LPS -induced ALI. beta-Actin was used as the reference gene. G , H ELISA was used to analyse the IL-1beta and IL-18 levels in the culture supernatants. I , J Cell apoptosis was determined by Hoechst 33342 and PI dual staining assays (I) and counted (J). K Western blotting was used to analyse the protein expression of NLRP3 and caspase-1 after lncRNA NLRP3 overexpression in the cytoplasm. The data are presented as mean \pm SE (n = 6). * P

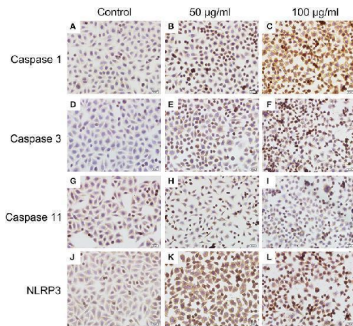


Schematic summarizes the mechanism that NLRP3 inflammasome activation in endothelium mediates hypertonic stress-induced atherosclerosis via NFAT5. Schematic illustration of the process. Stage i: Hypertonicity \rightarrow NFAT5-dependent NLRP3 gene transcription \rightarrow NLRP3 inflammasome activation. Stage ii: NLRP3 inflammasome activation \rightarrow NFAT5-transcription-mediated pro-IL-1beta \rightarrow IL-1beta secretion. Stage iii: IL-1beta secretion \rightarrow adhesive molecules \rightarrow monocytes adhesion and infiltration. Stage iv: The activation of endothelial innate immunity promotes macrophage-driven foam cells and phenotype conversion of smooth muscle cells, contributing to the formation of atherosclerosis Index in PubMed under a CC BY license. PMID: 31429763

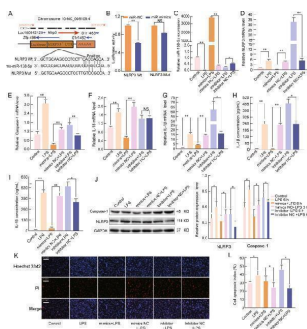
LncRNA NLRP3 functions as a sponge for miR-138-5p. A LncLocator was used to investigate the distribution of lncRNA NLRP3. B LncRNA NLRP3 was mainly located in the cytoplasm. C Venn diagram of miRDB predicting miR-138-5p and miR-370-3p sponged by lncRNA NLRP3 and NLRP3. D , E The predicted miR-138-5p-binding sites in the lncRNA NLRP3 3'-UTR. F miR-138-5p mimics notably reduced the luciferase activity of the lncRNA NLRP3-Wt group. G silncRNA NLRP3



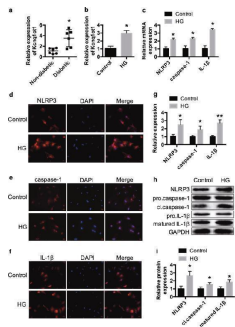
significantly increased miR-138-5p expression; however, overexpression of lncRNA NLRP3 reduced miR-138-5p expression in LPS-treated NR8383 AM cells. H RIP assays revealed that Ago2-containing beads enriched the expression of miR-138-5p and NLRP3. I The miR-138-5p inhibitor and miR-138-5p mimics had no effects on lncRNA NLRP3 expression in LPS-treated NR8383 AM cells. The data are presented as mean ± SE (n = 6). J lncRNA NLRP3 expression was negatively correlated with miR-138-5p expression in LPS-treated NR8383 AM cells. * P



Immunocytochemistry analysis of histone induced activations of caspase 1, caspase 3, and NLRP3 (400×). BMECs were cultured briefly on cover glasses (pre-treated with poly-L -lysine, 0.1 mg/mL, Sigma-Aldrich) and incubated with histone (50 and 100 ug/mL) for 16 h. The samples were visualized with DAB, counterstained with hematoxylin and observed by inverted microscope. Three independent experiments were carried out by light microscope analyses. Index in PubMed under a CC BY license. PMID: 31156617

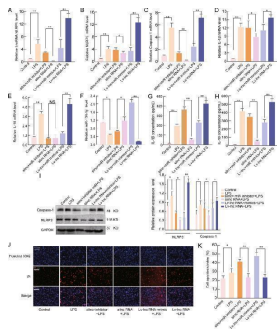


miR-138-5p regulates the inflammatory response by targeting NLRP3. A The predicted miR-138-5p-binding sites in the NLRP3 mRNA 3'-UTR. B A firefly luciferase reporter containing either wild-type or mutant NLRP3 was cotransfected into NR8383 AM cells with miR-138-5p mimics NC or miR-138-5p mimics. qRT-PCR assays were used to analyse the mRNA expression of C miR-138-5p, D NLRP3, E Caspase-1, F IL-18, and G IL-1beta in the NR8383 AM cells (n = 6). beta-Actin was used as a reference gene. H , I ELISA was used to analyse the IL-1beta and IL-18 levels in the culture supernatants. J Western blotting assay of the protein expression levels of NLRP3 and Caspase-1. K , L Cell apoptosis was determined by Hoechst 33342 and PI dual staining assays (K) and counted (L). The data are presented as mean ± SE (n = 6). * P

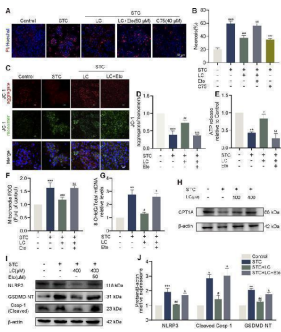


Kcnq1ot1 and pyroptosis are activated in HG-treated cardiac fibroblasts qRT-PCR was performed to measure the Kcnq1ot1 expression level in the serums of non-diabetic and diabetic patients a . * P

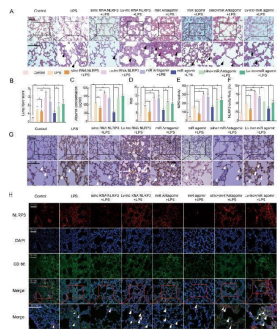
lncRNA NLRP3 regulates the inflammatory response through the lncRNA NLRP3/miR-138-5p/NLRP3 ceRNA network in vitro. miR-138-5p suppression reversed the effects of silncRNA NLRP3 on the mRNA expression of A lncRNA NLRP3, B NLRP3, C Caspase-1, D IL-1beta, E IL-18, and F miR-138-5p in NR8383 alveolar macrophage (AMs) cells. beta-Actin was



used as the reference gene. G , H ELISA analysis of the IL-1β and IL-18 levels in the culture supernatant. I Western blotting assay of the protein expression levels of NLRP3 and caspase-1. J , K Cell apoptosis was determined by Hoechst 33342 and PI dual staining assays (J) and counted (K). The data are presented as mean ± SE (n = 6). * P



LC protects against STC-induced acinar cell pyroptosis via CPT1A. (A,B) Representative images and quantification of Hoechst 33342 (blue) and PI (red) staining of primary acinar cells received different treatments. Scale bar: 50 μm. (C,D) JC-1 fluorescent staining of primary acinar cells in different treatment groups. Scale bar: 50 μm. (E) The release of ATP levels in the supernatant of cultured primary acinar cells received different treatments. (F) Quantification of mtROS in primary acinar cells in different treatment groups. (G) The ratio of 8-OHdG to total mtDNA content in primary acinar cells received different treatments. (H) Protein levels of CPT1A and beta-actin in the primary acinar cells received different treatments. (I,J) Protein levels of NLRP3, cleaved Caspase-1 and GSDMD-NT in the primary acinar cell received different treatments. beta-actin served as the loading control (n = 3). Data are presented as means ± SEM, n = 3-5. * p < 0.05, ** p < 0.01, *** p < 0.001 vs. Control group. # p < 0.05, ## p < 0.01, ### p < 0.001, vs. STC group. & p < 0.05, && p < 0.01, &&& p < 0.001 vs. STC+LC treatment group. STC: sodium taurocholate; LC: L-carnitine; Eto: Etomoxir. Index in PubMed under a CC BY license. PMID: 40718711



LncRNA NLRP3/miR-138-5p/NLRP3 functions via the ceRNA during the NLRP3-triggered inflammatory response in vivo. Rat lungs were injected with PBS in the control group and LPS-treated rats were further treated with si-r-lncRNA NLRP3, Lv-lncRNA NLRP3, agomiR-138-5p, antagonomiR-138-5p, Lv-lncRNA NLRP3 + agomiR-138-5p, and si-r-lncRNA NLRP3 + antagonomiR-138-5p. A Lung tissue samples were collected 6 h after establishing LPS-induced ALI to analyse the histopathological changes (×200, ×400). The black arrow indicates neutrophil infiltration, pulmonary oedema, alveolar wall thickening, and alveolar haemorrhage. B The lung injury score was determined via H&E staining, a representative histological analysis (n = 6 animals per group). C ELISA was used to measure the BALF albumin content. D Detection of the lung W/D ratio in rats. E MPO activity in the lung tissues of rats. F , G Immunohistochemical detection of the NLRP3 contents in rat lung tissues (×200, ×400). H The inflammatory response in NR8383 AM cells was suppressed by si-r-lncRNA NLRP3 and miR-138-5p mimics alone or in combination, as shown by the decreased number of cells colabeled with CD68 (green) and NLRP3 (red). LncRNA NLRP3 overexpression, miR-138-5p inhibition, and NLRP3 augmented the inflammatory response

in LPS-induced ALI with more NLRP3 and CD68 anchored in the plasma membrane of the AM cells. The data are presented as mean \pm SE (n = 6). * P

18 Publications Citing This Product

1. PubMed ID: 10.1016/j.cbi.2021.109572, Pelargonic acid vanillylamide and rosuvastatin protect against oxidized low-density lipoprotein-induced endothelial dysfunction by inhibiting the NF-kappaB/NLRP3 pathway and improving cell-cell junctions
2. PubMed ID: 10.1002/jbt.22978, The combination of dapagliflozin and statins ameliorates renal injury through attenuating the activation of inflammasome-mediated autophagy in insulin-resistant rats
3. PubMed ID: 34217687, Sivasinprasasn S,Wikan N,Tocharus J,Chaichompoo W,Suksamrarn A,Tocharus C.Pelargonic acid vanillylamide and rosuvastatin protect against oxidized low-density lipoprotein-induced endothelial dysfunction by inhibiting the NF-kappaB/NLRP3 pathway and improving cell-cell junctions.Chem Biol Interact.2021 Jul 1:109572.doi:10.1016/j.cbi.2021.109572.Epub ahead of print.PMID:34217687.

Visit bosterbio.com/anti-cias1-nalp3-antibody-pa1665-boster.html to see all 18 publications.

Submit a product review to Biocompare.com

Submit a review of this product to Biocompare.com to receive a \$20 Amazon.com giftcard! Your reviews help your fellow scientists make the right decisions. Thank you for your contribution.



Anti-CIAS1/NALP3/NLRP3 Antibody

For Research Use Only. Not for use in diagnostic procedures.